Received: 28 February 2018 | Revised: 24 May 2018 | Accepted: 2 July 2018

DOI: 10.1002/ese3.216

Energy Science & Engineering
Open Access

RESEARCH ARTICLE

Extraction of a photovoltaic cell's double-diode model parameters from data sheet values

Georg Sulyok | **Johann Summhammer**

Atominstitut, TU Wien, Vienna, Austria

Correspondence: Georg Sulyok, Atominstitut, TU Wien, 1020 Vienna, Austria (georg.sulyok@tuwien.ac.at).

Funding information
H2020 Industrial Leadership, Grant/Award Number: ID 737884; H2020 Societal Challenges, Grant/Award Number: ID 737884; H2020 Fast Track to Innovation, Grant/Award Number: ID 737884

Abstract

In the data sheets of photovoltaic cells, manufacturers usually only provide selected points of the cell's current-voltage curve, that is, short-circuit current, open-circuit voltage and current and voltage at the maximum power point. However, these three parameters do not suffice to deduce the cell's double diode model parameters. Thus, it is not possible to reproduce the complete current-voltage characteristics. Here, we point out how the range of the double diode parameters can be determined from the available data points and present approximately valid conditions which can be exploited to derive unique double diode parameter sets. The introduced methods rely on the solution of one-dimensional equations and the intervals within which their roots lie are established. Thus, a straightforward extraction of the parameters is possible. The reliability of four different methods is checked by comparison with real cells whose double diode parameters are known for varying temperature and illumination conditions as well as with numerically generated parameters. Accurate parameter guesses and a faithful reproduction of the cell's IV-curve can be achieved, in particular, for present-day high-quality cells.

KEYWORDS

double diode model, IV-curve reconstruction, parameter extraction, silicon PV cells

1 | INTRODUCTION

Energy consumption is continuously increasing worldwide and thus, in the sense of sustainability and environmentalism, focus on renewable energy sources has been strongly enhanced. As far as the exploitation of solar energy is concerned, the electricity-generating capacity of photovoltaics (PV) has experienced a considerable growth over the last decades[1] and the European Union established the objective of a 12% share of its total electricity demand until 2020.[1]

The fundamental building block of any PV-system is the solar cell. Being basically a diode whose p-n junction is exposed to light its functioning is explained in detail by semiconductor theory.[2,3] For practical purposes however, the microscopic processes are modeled by equivalent circuit diagrams allowing to obtain the cell's current-voltage characteristics (IV-curve) with sufficient accuracy and within reasonable calculational effort. Determining the parameters of the single cell's circuit model is essential for evaluation, dimensioning, and manufacturing of PV-modules and entire PV-systems. Moreover, the exact knowledge of the model parameters allows to draw conclusions about inner cell processes and can serve as starting point for further research and cell optimization.

In the literature, two lumped circuit models are prevalent, the single-diode model[4-7] and the two-diode model.[8-13] Obtaining the respective model parameters by fitting measured data points to the theoretical IV-curve is aggravated by

the fact that these IV-curves are given by nonlinear, implicit equations. Various refined techniques have been developed, reviewed in Ref.,[14] requiring full IV-curve data in the majority of cases. In some approaches,[8,9,15] the parameters are directly calculated using only selected data points. However, these methods necessitate the knowledge of slopes at short-circuit current[8,9] and at open-circuit voltage,[15] an information that is usually not provided by the manufacturer. In case of the single-diode model, methods to determine the model parameters from the limited information provided by manufacturer's data sheets have already been developed,[16,17] but require the solution of high-dimensional nonlinear equation systems. Here, we focus our investigations on the double-diode model, since for conventional silicon cells, it provides better accuracy in fitting measured data, especially in the vicinity of the maximum power point.[18,19] A first scheme for the double diode parameter extraction relying solely on data points available from cell data sheets (short circuit current, open circuit voltage, current and voltage at maximum power point) was presented by Ref.,[11] but suffers from some impracticalities and incompleteness of the analysis.

We reduce the two-dimensional equation system of[11] to a single equation and can thus specify what is possible to gain from the limited informations of the data sheet with certainty and where approximations become necessary. We present different methods to extract the double diode model parameter set from the key data points and show that for present day high-quality cells the reliability of the newly derived extraction schemes surpasses the approach of.[11]

The paper is organized as follows: First, the double-diode model is recapitulated and the equations derived from the data sheet values are solved. Then, approximations are presented which allow to uniquely determine the double-diode parameters. In the next sections, the methods are illustrated in a case study and tested for further real cells with known double-diode parameters under varying temperature and illumination conditions and for numerically generated parameter sets. Conclusive remarks and acknowledgments complete the contribution.

2 | DOUBLE-DIODE EQUATION

In Figure 1, the equivalent circuit of the double-diode model is shown. From Kirchhoff's nodal rule, the basic equation relating the cell's output current I and voltage V is given by

$$f(I,V) = I + I_{s_1}\left(e^{\frac{V+IR_s}{n_1 V_T}} - 1\right) + I_{s_2}\left(e^{\frac{V+IR_s}{n_2 V_T}} - 1\right) + \frac{V+IR_s}{R_{sh}} - I_{ph} = 0 \quad (1)$$

where I_{ph} denotes the photo current, I_{s_1} and n_1 stand for the saturation current and ideality factor of the first diode, I_{s_2} and n_2 stand for the saturation current and ideality factor of the second diode, R_s and R_{sh} account for serial and parallel resistances, and V_T is the thermal voltage defined as $V_T = k_B T/e$ where k_B is the Boltzmann constant ($\approx 1.38\times10^{-19}$ J/K), e is the elementary charge ($\approx 1.6\times10^{-19}$ C), and T is the p-n junction's absolute temperature. The first diode models the diffusion current and the second diode takes recombination currents into account. Thus, according to Shockley's diffusion theory,[20,21] we can set the ideality factors $n_1 = 1$ and $n_2 = 2$ in Equation (1). The possibility of directly relating physical processes inside the cell and corresponding efficiency loss mechanisms with model parameters is another reason for choosing the more elaborate double-diode model instead of the single-diode model.

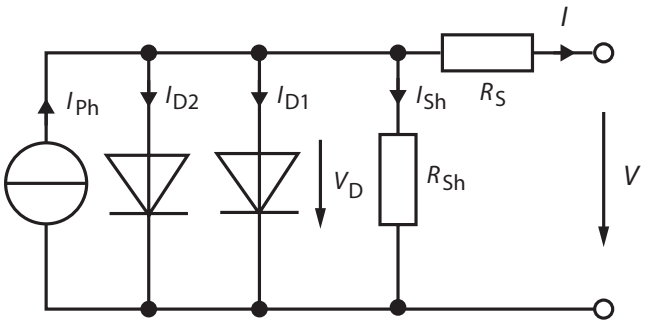

FIGURE 1 Equivalent circuit diagram of the solar cell's double diode model

The remaining five parameters (R_s,R_{sh},I_{ph},I_{s_1},I_{s_2}) shall now be recovered from data sheet information only, that is, from short-circuit current (I_{sc}), open-circuit voltage (V_{oc}) and current and voltage at maximum power point (I_m and V_m). These parameters fulfill Equation (1) such that

$$f(0,V_{oc}) = 0 \quad (2)$$

$$f(I_m,V_m) = 0 \quad (3)$$

$$f(I_{sc},0) = 0 \quad (4)$$

from which we can evaluate

$$I_{ph} = \frac{V_{oc}}{R_{sh}} + I_{s_1}\left(A_{oc}^2 - 1\right) + I_{s_2}\left(A_{oc} - 1\right) \quad (5)$$

$$I_{s_1} = \frac{a - I_{s_2}(A_{oc} - A_{sc})}{A_{oc}^2 - A_{sc}^2} \quad (6)$$

$$I_{s_2} = \frac{b(A_{oc}^2 - A_{sc}^2) - a(A_m^2 - A_{sc}^2)}{(A_m - A_{oc})(A_m - A_{sc})(A_{sc} - A_{oc})} \quad (7)$$

where

$$A_{oc} = \exp\left(\frac{V_{oc}}{2V_T}\right), \quad A_{sc} = \exp\left(\frac{I_{sc}R_s}{2V_T}\right) \quad (8)$$

$$A_{\mathrm{m}} = \exp\left(\frac{V_{\mathrm{m}} + I_{\mathrm{m}} R_{\mathrm{s}}}{2V_{\mathrm{T}}}\right) \tag{9}$$

$$a = I_{\mathrm{sc}}\left(1 + \frac{R_{\mathrm{s}}}{R_{\mathrm{sh}}}\right) - \frac{V_{\mathrm{oc}}}{R_{\mathrm{sh}}} \tag{10}$$

$$b = (I_{\mathrm{sc}} - I_{\mathrm{m}})\left(1 + \frac{R_{\mathrm{s}}}{R_{\mathrm{sh}}}\right) - \frac{V_{\mathrm{m}}}{R_{\mathrm{sh}}} \tag{11}$$

Thus, using equations (2-4), three of the five parameters have been eliminated and I_{ph}, I_{s_1}, and I_{s_2} can be expressed as functions of R_{s} and R_{sh}. From $P = I \cdot V$, the derivative of $I(V)$ at the maximum power point (MPP) can be deduced

$$\frac{dP}{dV} = \frac{dI}{dV}V + I \rightarrow \frac{dI}{dV}|_{\mathrm{MPP}} = -\frac{I_{\mathrm{m}}}{V_{\mathrm{m}}} \tag{12}$$

yielding the fourth condition contained in the data sheet values

$$\frac{df(I,V)}{dV}|_{\mathrm{MPP}} = 0 \tag{13}$$

Implicit differentiation of Equation 1 gives

$$\frac{dI}{dV} = -\frac{D}{1 + R_{\mathrm{s}}D} \tag{14}$$

with

$$D = \frac{1}{R_{\mathrm{sh}}} + \frac{I_{\mathrm{s}_1}}{V_{\mathrm{T}}}e^{\frac{V+IR_{\mathrm{s}}}{V_{\mathrm{T}}}} + \frac{I_{\mathrm{s}_2}}{2V_{\mathrm{T}}}e^{\frac{V+IR_{\mathrm{s}}}{2V_{\mathrm{T}}}} \tag{15}$$

Inserting the values at MPP, condition Equation 13 reads

$$\frac{I_{\mathrm{m}}}{V_{\mathrm{m}}} = \left(1 - R_{\mathrm{s}}\frac{I_{\mathrm{m}}}{V_{\mathrm{m}}}\right)\left(\frac{1}{R_{\mathrm{sh}}} + \frac{I_{\mathrm{s}_1}}{V_{\mathrm{T}}}A_{\mathrm{m}}^2 + \frac{I_{\mathrm{s}_2}}{2V_{\mathrm{T}}}A_{\mathrm{m}}\right) \tag{16}$$

where A_{m} is taken from Equation 9. Using I_{s_1} (Equation 6) and I_{s_2} (Equation 7) in Equation (16) it is possible to express R_{sh} as

$$R_{\mathrm{sh}} = \frac{1 + q + s}{\frac{I_{\mathrm{m}}}{cV_{\mathrm{m}}} - p - r} \tag{17}$$

where

$$q = \frac{hA_{\mathrm{m}}^2}{V_{\mathrm{T}}}, s = \frac{lA_{\mathrm{m}}}{2V_{\mathrm{T}}}, p = \frac{gA_{\mathrm{m}}^2}{V_{\mathrm{T}}}, r = \frac{kA_{\mathrm{m}}}{2V_{\mathrm{T}}} \tag{18}$$

$$c = 1 - R_{\mathrm{s}}\frac{I_{\mathrm{m}}}{V_{\mathrm{m}}} \tag{19}$$

$$h = \frac{d - (A_{\mathrm{oc}} - A_{\mathrm{sc}})l}{A_{\mathrm{oc}}^2 - A_{\mathrm{sc}}^2} \tag{20}$$

$$l = \frac{e(A_{\mathrm{oc}}^2 - A_{\mathrm{sc}}^2) - d(A_{\mathrm{m}}^2 - A_{\mathrm{sc}}^2)}{N} \tag{21}$$

$$d = I_{\mathrm{sc}}R_{\mathrm{s}} - V_{\mathrm{oc}}, \quad e = (I_{\mathrm{sc}} - I_{\mathrm{m}})R_{\mathrm{s}} - V_{\mathrm{m}} \tag{22}$$

$$N = (A_{\mathrm{m}} - A_{\mathrm{oc}})(A_{\mathrm{m}} - A_{\mathrm{sc}})(A_{\mathrm{sc}} - A_{\mathrm{oc}}) \tag{23}$$

$$g = \frac{I_{\mathrm{sc}} - (A_{\mathrm{oc}} - A_{\mathrm{sc}})k}{A_{\mathrm{oc}}^2 - A_{\mathrm{sc}}^2} \tag{24}$$

$$k = \frac{(I_{\mathrm{sc}} - I_{\mathrm{m}})(A_{\mathrm{oc}}^2 - A_{\mathrm{sc}}^2) - I_{\mathrm{sc}}(A_{\mathrm{m}}^2 - A_{\mathrm{sc}}^2)}{N} \tag{25}$$

With the above abbreviations, we can write I_{s_1} and I_{s_2} as

$$I_{\mathrm{s}_1} = g + \frac{h}{R_{\mathrm{sh}}}, \quad I_{\mathrm{s}_2} = k + \frac{l}{R_{\mathrm{sh}}} \tag{26}$$

which proves to be beneficial when using the algorithm in practice. Note, that R_{sh} (Equation 17) is a function of R_{s} only which also holds for I_{s_1}, I_{s_2}, and I_{ph} if R_{sh} is inserted. Thus, as to be expected, four of the five unknown parameters are determined by the conditions imposed by Equations (2-4) and Equation 13.

To delimit the possible range of the remaining free parameter R_{s} additional physical constraints can be exploited. Diode saturation currents and ohmic resistances have positive values. Thus, the zeros of R_{sh}, I_{s_2}, and I_{s_1} (being functions of R_{s}) have to be determined.

We start with I_{s_2} and search for a root in the interval $R_{\mathrm{s}} \in [0, (V_{\mathrm{oc}} - V_{\mathrm{m}})/I_{\mathrm{m}}]$. The choice of the upper bound can be argued from

$$R_{\mathrm{s}} < -\frac{1}{I'(V_{\mathrm{oc}})} < \frac{V_{\mathrm{oc}} - V_{\mathrm{m}}}{I_{\mathrm{m}}} \tag{27}$$

where the first inequality is derived from Equation 14 recognizing that D is a positive number. The second inequality holds since the tangent of $I(V)$ at V_{oc} is steeper than the secant intersecting $(V_{\mathrm{m}}, I_{\mathrm{m}})$ and $(V_{\mathrm{oc}}, 0)$. The obtained root constitutes an upper limit $R_{\mathrm{s}}^{\mathrm{upp}}$ for R_{s} since I_{s_2} becomes negative when R_{s} is further increased. Alternatively, the case $I_{\mathrm{s}_2} = 0$ can be seen as switching to the single-diode model (with diode ideality factor n = 1) whose R_{s} must be larger than the serial resistance of the double-diode model to result in the same circuit parameters $(V_{\mathrm{oc}}, I_{\mathrm{sc}}, V_{\mathrm{m}}, I_{\mathrm{m}})$.

Since I_{s_1} monotonously increases for $R_{\mathrm{s}} \in [0, R_{\mathrm{s}}^{\mathrm{upp}}]$ checking the sign of $I_{\mathrm{s}_1}(0)$ is sufficient to ensure the positivity of I_{s_1}. Only if $I_{\mathrm{s}_1}(0) < 0$ a root exists which has to be determined numerically yielding a lower limit $R_{\mathrm{s}}^{\mathrm{low}}$ for R_{s}, otherwise $R_{\mathrm{s}}^{\mathrm{low}} = 0$.

In most cases, I_{s_1} does not supply a lower limit different from zero. A restriction coming into effect more frequently is provided by the shunt resistance's positivity. The sign change of R_{sh} does not happen continuously but at a pole of R_{sh}. Therefore, the root of the inverse $1/R_{\mathrm{sh}}$ has to be determined

within $[R_s^{low},R_s^{upp}]$. The obtained value of R_s serves as new lower bound R_s^{low} for the actual double diode model's R_s. If there's no root in $[R_s^{low},R_s^{upp}]$ the lower bound for R_s remains unaltered.

Since the positivity of the other parameters is ensured for $R_s \in [R_s^{low},R_s^{upp}]$, the photo current I_{ph} fulfills $I_{ph} > I_{sc}$ as can be checked from Equation 4. I_{ph} therefore provides no further restriction on the possible range of R_s.

3 | APPROXIMATE CONDITIONS

Any serial resistance $R_s \in [R_s^{low},R_s^{upp}]$ together with the corresponding R_{sh} (Equation 17), I_{s_2} (Equation 7), I_{s_1} (Equation 6), and I_{ph} (Equation 5) forms a physically meaningful set of double diode parameters reproducing the input circuit parameters (V_{oc},I_{sc},V_m,I_m). Without further consideration, one could therefore readily chose for example the arithmetic mean $R_s^{half} \equiv (R_s^{upp}+R_s^{low})/2$ as R_s to be consistent with the data sheet specifications. We will call this approach R_s^{half} method.

For reasons that will be explained in more detail in chapter 1, we will also investigate the parameter set arising from the lowest possible serial resistance which will consequently be called R_s^{low}-method.

Aside from randomly choosing a serial resistance within $[R_s^{low},R_s^{upp}]$, one could also try to find an additional, fifth condition to determine R_s. In,[11] an approximate expression for the slope of the IV-curve at $V=0$ is used

$$\frac{dI}{dV}|_{V=0} \approx -\frac{1}{R_{sh}} \tag{28}$$

which can be applied to Equation 14 to yield the condition

$$0 = (R_{sh}-R_s)\left(\frac{1}{R_{sh}} + \frac{I_{s_1}}{V_T}e^{\frac{I_{sc}R_s}{V_T}} + \frac{I_{s_2}}{2V_T}e^{\frac{I_{sc}R_s}{2V_T}}\right) \equiv C^{1/R_{sh}} \tag{29}$$

Inserting the explicit expressions of R_{sh} (Equation 17), I_{s_1} (Equation 6), and I_{s_2} (Equation 7) gives a nonlinear equation for R_s whose solution uniquely determines the double diode model parameter set.

It is worth noting that the determination of the double diode parameters using Equation 28 gives the same numerical values as the method of,[11] but the algorithm of the present work differs in various aspects. In,[11] R_{sh} is not explicitly expressed as function of R_s from Equation (16), but a two-dimensional equation system for R_{sh} and R_s consisting of Equations (16) and (28) is solved with the Newton-Raphson method. Finding convergent initial values for both R_{sh} and R_s is therefore essential and requires some effort and case distinctions. We prefer the single equation for R_s whose roots are restricted to a finite range by physical considerations and can then determined by bracketing procedures (eg, bisection or Brent's method).

The authors of[11] also use the approximation $e^{V_{oc}/(n_i V_T)} >> e^{R_s I_{sc}/(n_i V_T)}$, $i=1,2$ from[15] which considerably simplifies the expressions for I_{s_1}, I_{s_2}, and Equations (16) and (28). Since the nonlinear equation for R_s anyway can only be solved numerically we do not apply these approximations. Moreover, though not mentioned in Ref.,[11] the two-dimensional equation system exhibits a trivial solution for $R_s = (V_{oc}-V_m)/I_m$ and arbitrary R_{sh} which has to be considered an artifact of the above approximations.

Determining a unique value of R_s relied on demanding the approximate condition Equation (28) to be exactly fulfilled. In what follows, we will refer to this approach as $1/R_{sh}$-method. One may assume that other approximate conditions can also be used to determine R_s. We therefore consider the following: In the double-diode model as described by Equation (1), the IV-curve $I(V)$ and its derivative $I'(V)$ are monotonously decreasing. Thus, the slope of a secant is bounded by the slope of the tangents at its intersection points, that is, for $V_1 < V_2$

$$I'(V_1) \geq \frac{I(V_1)-I(V_2)}{V_1-V_2} \geq I'(V_2) \tag{30}$$

In the nearly linear regime of the IV-curve around $V=0$ we can approximate

$$\frac{I(V_1)-I(V_2)}{V_1-V_2} \approx \frac{I'(V_1)+I'(V_2)}{2} \tag{31}$$

For $V_1 = -I_{ph}R_s$, $I(-I_{ph}R_s) = I_{ph}$ and $V_2 = 0$, $I(0) = I_{sc}$ we get

$$\frac{I_{ph}-I_{sc}}{-I_{ph}R_s} \approx \frac{I'(-I_{ph}R_s)+I'(0)}{2} \tag{32}$$

Although this approximation is usually very well fulfilled for all $R_s \in [R_s^{low},R_s^{upp}]$, it turns out that reaching an exact equality is often impossible. However, exchanging I_{ph} in the denominator of the left hand side with I_{sc} results in a solvable condition for R_s within the physically allowed range

$$0 = \frac{I'(-I_{ph}R_s)+I'(0)}{2}\frac{-I_{sc}R_s}{I_{ph}-I_{sc}} \equiv C^{2tan} \tag{33}$$

which we denote 2tangs-method.

Using Equation (14) the derivatives are explicitly given by

$$I'(-I_{ph}R_s) = \frac{-N_1}{1+R_sN_1}, \quad I'(0) = \frac{-N_2}{1+R_sN_2} \tag{34}$$

with

$$N_1 = \frac{1}{R_{sh}} + \frac{I_{s_1}}{V_T} + \frac{I_{s_2}}{2V_T} \tag{35}$$

$$N_2 = \frac{1}{R_{sh}} + \frac{I_{s_1}}{V_T} A_{sc}^2 + \frac{I_{s_2}}{2V_T} A_{sc} \tag{36}$$

Inserting these expressions into Equation (33) together with the formulas for R_{sh} (Equation 17), I_{s_1} (Equation 6), I_{s_2} (Equation 7), and I_{ph} (Equation 5) we obtain a nonlinear equation determining R_s.

It has to be noted that different approximations involving the derivative of the IV-curve, for example simply equating the slope of the secant with the slope of the IV-curve at $V = 0$, are conceivable, but condition Equation (33) yielded the best results when testing the algorithms.

4 | CASE STUDY

To illustrate and compare the parameter extraction schemes, we apply them to the S'tile sunrays quarter cell, a 39 × 156 mm2 multicrystalline silicon PV cell. The IV-curve consisting of about 60 points (see Figure 2) was recorded under standard testing conditions (STC, cell temperature of 25°C and an irradiance of 1000 W/m2 with an air mass 1.5 spectrum) and has been kindly provided by the S'tile company, Poitiers, France.

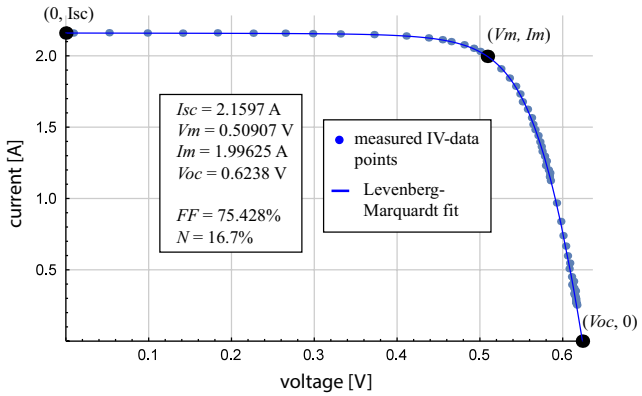

FIGURE 2 IV-curve (data points + fit), circuit parameters, fill factor (FF) and efficiency (N) of the case study cell (S'tile sunrays quarter cell) at standard testing conditions

From the full curve we can extract the double diode parameters by a Levenberg-Marquart fit. All data points are equally weighted in the fit routine since their measurement uncertainties can be assumed to be of the same order of magnitude. The optimal parameter set is thus determined by minimizing the quadratic distances of the theory curve to the measured data points. The normalized root mean square error percentage (nRMSE [%]) is given by

$$\text{nRSME}\,[\%] = \frac{\sqrt{\frac{1}{N}\sum_{i=1}^{N}(t_i - m_i)^2}}{\sqrt{\frac{1}{N}\sum_{i=1}^{N} m_i^2}} \times 100 \tag{37}$$

where N is the number of data points, m_i are the measured values and t_i the theoretically expected values. As shown in Table 1, the double diode parameters obtained from the fit routine indeed give the lowest nRMSE. From these optimal double diode parameters, the circuit parameters (V_{oc},I_{sc},V_m,I_m) can be calculated and used as input for the extraction algorithms. The quality of the different extraction methods will be judged by how close each of them can reproduce the underlying "optimal" double diode parameters.

By inserting the circuit parameters (V_{oc},I_{sc},V_m,I_m) into Equations (26), (17), and (5), I_{s_2}, I_{s_1}, R_{sh}, and I_{ph} can be expressed as functions of R_s only. In Figure 3, we display the graphs of these functions. I_{s_2} is plotted from zero to $(V_{oc} - V_m)/I_m = 57.49\,\text{m}\Omega$ and exhibits a root at $R_s = 19.11\,\text{m}\Omega$ serving as upper bound R_s^{upp}. I_{s_1} is positive within the range $[0, R_s^{upp}]$ and does therefore not contribute to a restriction on R_s. The shunt resistance R_{sh} however possesses a pole at $R_s = 13.28\,\text{m}\Omega$ which defines the physical lower bound R_s^{low}.

Remarkably, R_{sh} decreases with increasing R_s within the physically allowed range. Low serial/high shunt resistance pairs yield the same circuit parameters and the same fill

TABLE 1 Double diode parameters, root mean square deviations from the measured data points, and error measures E_1 and E_2 of the different extraction schemes applied to the S'tile quarter cell

	Full IV-curve	R_s^{half}	$1/R_{sh}$	2tangs	R_s^{low}
Parameters					
R_s [mΩ]	14.00	16.19	16.80	14.20	13.28
R_{sh} [Ω]	103.3	21.8	17.2	79.3	∞
I_{ph}[A]	2.160	2.161	2.162	2.160	2.160
I_{s_1}[nA]	0.0453	0.0509	0.0529	0.0458	0.0434
I_{s_2}[μA]	3.02	1.80	1.44	2.91	3.40
Errors					
nRSME [%]	1.13	1.57	1.90	1.14	1.15
E_1 [%]	0.0	29.63	34.54	5.9	∞
E_2[‰]	0.0	2.05	2.70	0.17	0.58

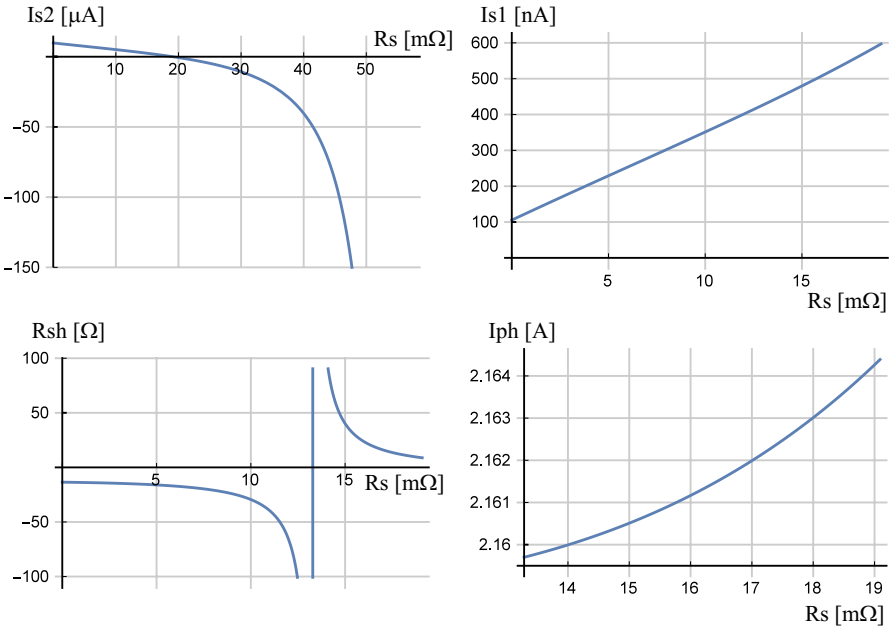

FIGURE 3 Double diode parameters I_{s_2}, I_{s_1}, R_{sh}, and I_{ph} as function of R_s for the circuit parameters $I_{sc} = 2.1597A$, $V_m = 0.509V$, $I_m = 1.996A$, and $V_{oc} = 0.624V$ of the S'tile sunray quarter cell at STC. Positivity of all parameters restricts R_s to lie between 13.28 and 19.11 mΩ

factor as high serial/low shunt resistance pairs. This counterintuitive behavior is compensated by an increased photo current I_{ph} and a decreased recombination current I_{s_2} for the high serial/low shunt resistance case.

In the R_s^{half}-method, R_s is set to $(R_s^{low} + R_s^{upp})/2 = 16.2\,\text{m}\Omega$ and the remaining double diode parameters are calculated from Equations (17) and (5-7). The results are listed in Table 1.

To get the parameter set of the $1/R_{sh}$-method the root of Equation (29) for $R_s \in [R_s^{low} + \epsilon, R_s^{upp}]$ has to be determined. To avoid numerical problems due to the pole of R_{sh} at $R_s = R_s^{low}$ we increased the lower bound of the search interval by a small positive real number $\epsilon = 10^{-12}$. Bisection yields the root $R_s = 16.8\,\text{m}\Omega$ (see left panel of Figure 4) which fixes the rest of the parameters given in Table 1.

For the 2tangs-method, the root of Equation (33) has to be determined. It is given by $R_s = 14.2\,\text{m}\Omega$ (see right panel of Figure 4) and the related remaining double diode parameters are listed in Table 1.

The $1/R_{sh}$-method gives a serial resistance above R_s^{half} whereas the root of the 2tangs-methods lies below R_s^{half} near the lowest possible value of R_s. For the investigated cell, the 2tangs-method yields double-diode parameters closer to the ones obtained from the full IV-curve. The quality of the parameter reproduction can be evaluated by the mean relative distance between derived (p_i) and full IV-curve $(p_i^{(full)})$ parameters which we denote as error E_1

$$E_1 = \frac{1}{5}\sum_{i=1}^{5}\frac{|p_i - p_i^{(full)}|}{p_i^{(full)}}, \quad p_i = \{R_s, R_{sh}, I_{ph}, I_{s_1}, I_{s_2}\} \tag{38}$$

Since changes in the parameters are not linearly reflected by the curve we also introduce another error measure E_2. It is evaluated from the difference between the IV-curves calculated from the reproduced parameters $(I(V))$ and the full curve fit $(I^{(full)}(V))$. The behavior near the maximum power point (roughly $V_m \pm 10\%$) is of particular interest, for example when calculating the maximum power point for an entire module consisting of an arbitrary number of serially or parallel connected cells. We define

$$E_2 = \frac{1}{0.2V_m}\int_{0.9V_m}^{1.1V_m}\left|\frac{I(V) - I^{(full)}(V)}{I^{(full)}(V)}\right| dV \tag{39}$$

which gives the mean relative distance between the points of the full IV-data fitted curve and the curve from the

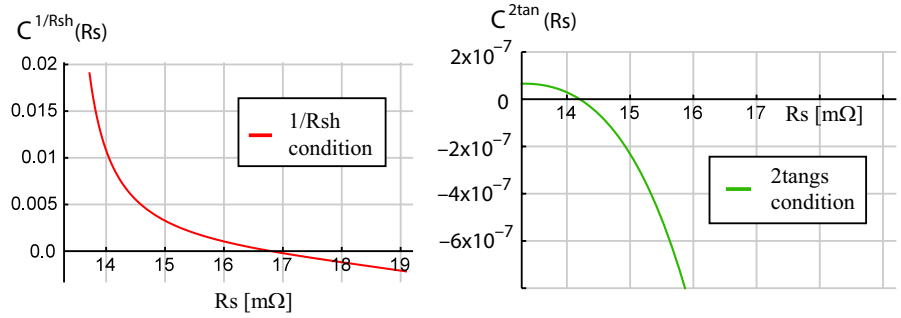

FIGURE 4 Approximate conditions for the circuit parameters $I_{sc} = 2.16A$, $V_m = 0.509V$, $I_m = 1.996A$, and $V_{oc} = 0.624V$ of the S'tile sunray quarter cell at STC: $1/R_{sh}$-method as given by Equation (29) (left panel), 2tangs-method Equation (33) (right panel)

reproduced parameters. For the investigated cell, the second error measure of the 2tangs-method lies one order of magnitude below the results for the R_s^{half}- and $1/R_{sh}$-method (see last row of Table 1).

5 | EVALUATION OF THE EXTRACTION SCHEMES

5.1 | Real cell data

It cannot be guaranteed that the results of the case study are representative for the majority of PV cells. To reach a more objective conclusion we use already published double-diode model parameters[10,15,22] to further test the algorithms. From these "official" double diode parameters, the electrical circuit parameters are deduced which serve as input for the extraction methods. The approximated double diode values are calculated and compared to the original ones. The general scheme is depicted in Figure 5. The two error measures E_1 and E_2 defined in the previous chapter quantify the quality of the different methods. The published double diode parameters have to be taken as reference quantities $p_i^{(full)}$ in Equation (38). The IV-curve $I^{(full)}(V)$ in Equation (39) is calculated from the published double diode parameters as well.

In,[10] a 2×2 cm2 silicon cell was investigated for different illumination levels (40%, 100%, and 140% of AM1) and temperatures (299.4∘K, 317.5∘K, and 330∘K). The full results are given in the appendix and allow the conclusion that the qualification of an extraction method for a particular cell is not influenced by temperature or illumination conditions.

In,[22] double diode parameters for three different commercial cells measured under standard testing conditions are listed. In,[15] double diode parameters for different cells at T = 323.15∘K under AM1 illumination are given. In addition, mono- and multicrystalline cells available at our research facility were measured under standard testing conditions and the double diode parameters were derived from a fitting procedure as described in the case study. The results of all these investigations for a total number of 16 cells are summarized in Figures 6 and 7.

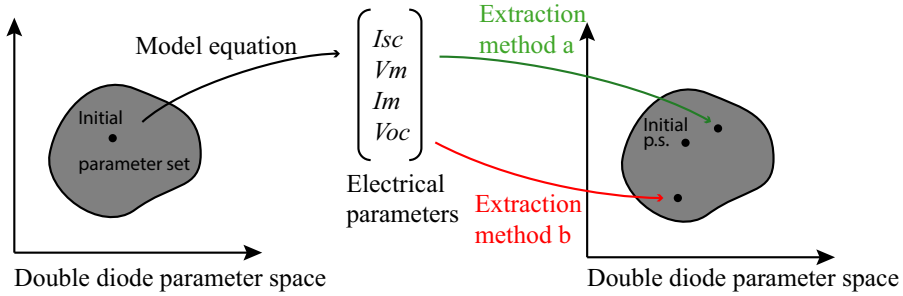

FIGURE 5 General scheme for judging the quality of a parameter extraction algorithm: Initial double diode parameters are obtained either from literature or complete IV-curve fits. Using Equation (1), the basic equation of the double diode model, the electrical circuit parameters (V_{oc},I_{sc},V_m,I_m) can be calculated which serve as input for the extraction methods. Each method yields different double diode parameters and the proximity to the original set indicates the reproduction quality

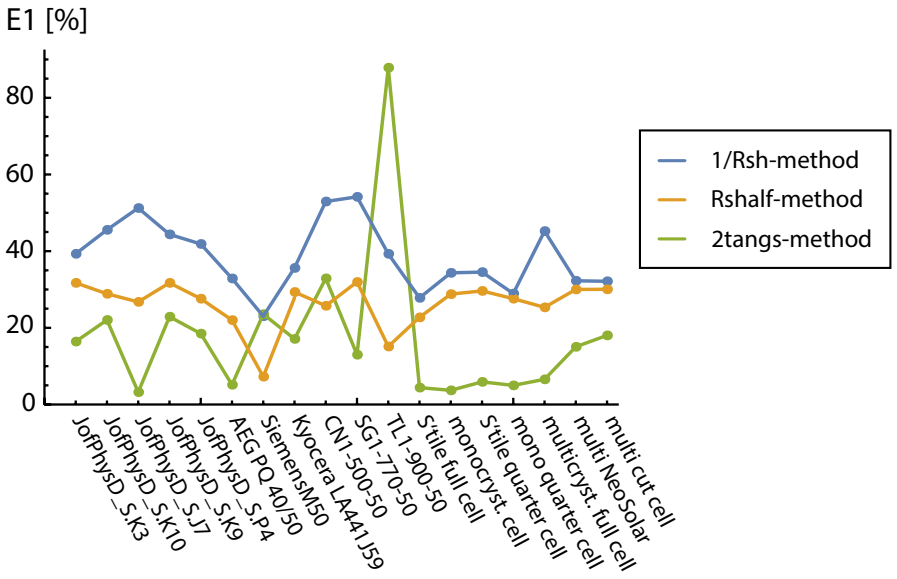

FIGURE 6 Parameter reproduction error E_1 (Equation 38) for cells with double diode parameters obtained from literature[10,15,22] or full IV-curve measurements

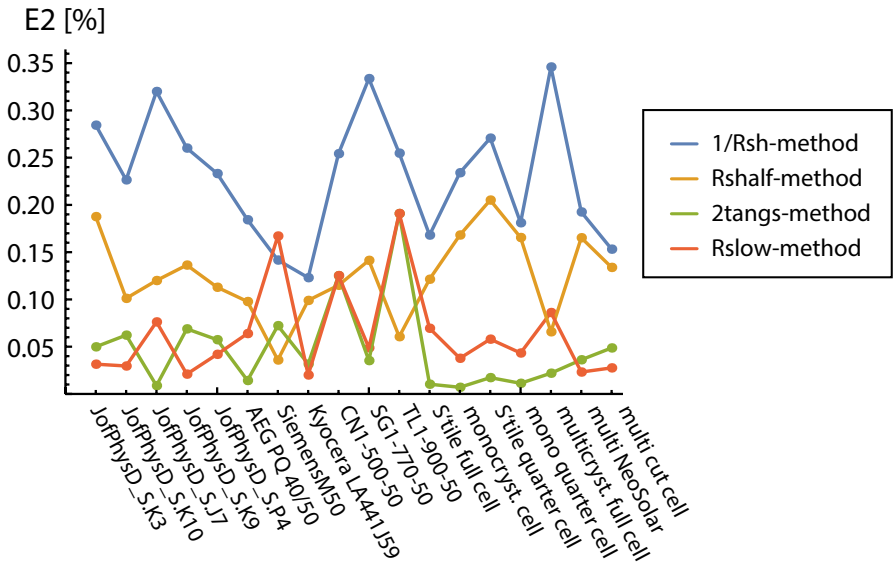

FIGURE 7 IV-curve reproduction error E_2 (Equation 39) for cells with double diode parameters obtained from literature[10,15,22] or full IV-curve measurements

The mean values of errors E_1 and E_2 displayed in Table 2. It can be concluded that the best parameter reproduction is achieved by the 2tangs-method. The only exception is the TL1-900-50 cell from.[15] It is therefore investigated in detail in Appendix B revealing that the double diode parameters obtained from the 2tangs-method are practically identical to the parameters of the R_s^{low}-method. In such cases, the parameters from the 2tangs-method have to be treated with care and it is recommended to switch to the R_s^{half} parameters. Despite the worse parameter reproduction, the deviation of the IV-curve (error measure E_2) is still below that of the $1/R_{sh}$-method. It can be assumed that the double diode parameter sets belonging to lower R_s still give good IV-curves, even if the parameter guess is inaccurate. This observation motivated us to include the R_s^{low}-method in our investigations. The R_s^{low}-method requires just as much effort as the R_s^{half}-method since no fifth equation has to be solved. Obviously, it performs badly if quantified by error measure E_1 since it yields an infinite shunt resistance R_{sh} for the majority of cells. Nevertheless, if the value of the parameters is irrelevant and if only a reliable IV-curve is required the quality of results is comparable to the 2tangs-method for our investigated cells (see Table 2).

5.2 | Numerically generated parameters

The number of available real cell data is limited and still rather low. A single outlier already caused a high standard deviation of the 2tangs-method's error measure E_1 (see Table 2). Therefore, we also generated cells numerically. Data from the real cell are used to estimate meaningful boundaries for double diode parameters of 156 × 156 mm2 cells under standard temperature and illumination conditions (see Table 3).

A parameter set randomly generated within these boundaries is accepted if the derived fill factor exceeds 70% as can be expected from commercially produced crystalline silicon solar cells. The corresponding circuit parameters are fed into the different parameter extraction schemes.

TABLE 2 Parameter extraction for 16 real cells, average errors of the different extraction schemes

Error	R_s^{half}	$1/R_{sh}$	2tangs	R_s^{low}
E_1 [%]	26.2 ± 6.3	38.6 ± 8.9	17.9± 19.4	∞
E_2[‰]	1.24± 0.45	2.31± 0.66	0.48± 0.47	0.65± 0.50

TABLE 3 Bounds for the randomly generated double diode parameter sets of 156 × 156 mm2 silicon cells under STC (AM1.5, 1000 W/m2, 25∘C)

Parameter	Range	Parameter	Range
R_s	1-50 mΩ	I_{s_1}	0.01-5 nA
R_{sh}	5-500 Ω	I_{s_2}	1-50 μA
I_{ph}	7-9 A		

Histograms of the two error measures for 10 000 generated parameter sets are shown in Figures 8 and 9. Mean value and standard deviation are listed in Table 4.

The histograms and average performances allow no statements about the reliability of an extraction method for an actual parameter set. We therefore also provide probabilities for the error of an extraction scheme to lie below the error of the other schemes. In Table 5 we compare error measures E_1 and in Table 6 error measures E_2. For example, the second entry in the first row of Table 5 indicates that for 9966 of the 10 000 generated double diode parameter sets the error measure E_1 of the R_s^{half}-method was smaller than the error measure E_1 of the $1/R_{sh}$-method.

It can be concluded that the low cost R_s^{half}-method already surpasses the $1/R_{sh}$-method, both for parameter (error E_1) and

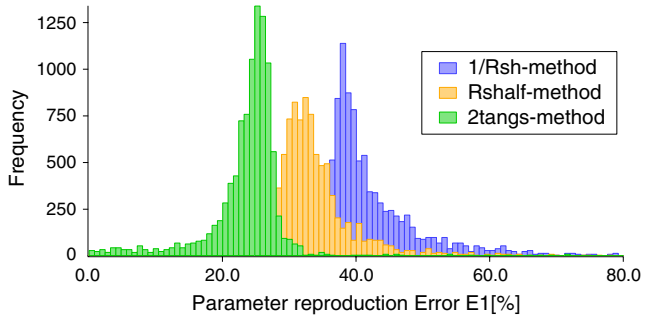

FIGURE 8 Histograms of the parameter reproduction error E_1 (Equation 38) for 10 000 numerically generated cells

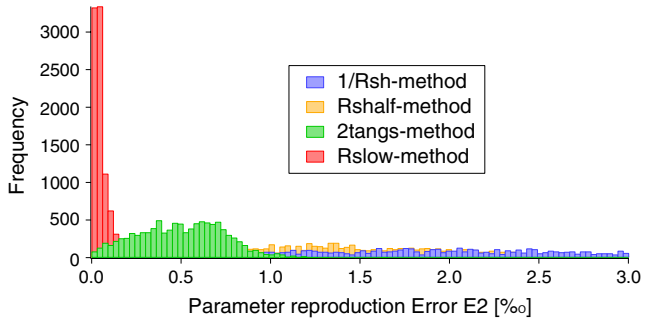

FIGURE 9 Histograms of the IV-curve reproduction error E_2 (Equation 39) for 10 000 numerically generated cells

TABLE 4 Mean values of the parameter reproduction errors of the different extraction schemes for 10 000 numerically generated cells

Error	R_s^{half}	$1/R_{sh}$	2tangs	R_s^{low}
E_1 [%]	32.8 ± 9.7	42.7 ± 12.8	24.1 ± 11.3	$\infty \pm \infty$
E_2[‰]	1.29 ± 0.78	2.14 ± 1.26	0.50 ± 0.24	0.10 ± 0.20

TABLE 5 Comparison of error E_1 for numerically generated cells

$P(E_1(x) > E_1(y))$ [%]		x: R_s^{half}	$1/R_{sh}$	2tangs	R_s^{low}
y:	R_s^{half}	—	99.66	5.59	99.98
	$1/R_{sh}$	0.34	—	0.86	99.94
	2tangs	94.41	99.14	—	99.99
	R_s^{low}	0.02	0.06	0.01	—

TABLE 6 Comparison of error E_2 for numerically generated cells

$P(E_2(x) > E_2(y))$ [%]		x: R_s^{half}	$1/R_{sh}$	2tangs	R_s^{low}
y:	R_s^{half}	—	99.69	5.16	3.34
	$1/R_{sh}$	0.31	—	0.39	1.1
	2tangs	94.84	99.61	—	6.12
	R_s^{low}	96.66	98.90	93.88	—

IV-curve (error E_2) reproduction. The reproduction quality can be further improved using the 2tangs-method which outdoes the R_s^{half}-method. It has to be noted that in the rare cases (less than 1‰) where multiple roots occurred for the 2tangs-method we took the largest one for R_s. Despite the good performance of the 2tangs-method, for reproducing the original IV-curve, the R_s^{low}-method beats all the other approaches, but behaves badly as far as parameter reproduction is concerned.

From investigating both real and numerically generated cells the following observations from the case study can be confirmed: The conditions provided by the electrical circuit parameters can be used to express R_{sh}, I_{ph}, I_{s_1}, and I_{s_2} as functions of R_s whose roots can be found numerically. Within the physically allowed range of R_s thereby determined, shunt resistance and recombination current decrease with increasing R_s, photo current and saturation current increase. The 2tangs-method yields a serial resistance in the lower range of the physically allowed values accompanied by high, but still realistic shunt resistance whereas the serial resistance obtained from the $1/R_{sh}$-method usually lies in the upper range of the spectrum and goes along with a lower shunt resistance. Cell design is no trivial task and not all cell parameters can be independently optimized. However, shunt resistances typically arise from the non-ideal manufacturing process and grown-in material defects,[23] rather than poor solar cell design. Therefore, the higher shunt resistances values obtained from the 2tangs-method can be assumed to be closer to the actual parameters for present-day cells.

6 | CONCLUSION

The present work was motivated by a straightforward task: Gaining access to the full current-voltage characteristics of a photovoltaic cell from the limited informations provided by the manufacturer's data sheet. While in case of the single diode model for photovoltaic cells a complete solution has already been published, the double diode model, which is more accurate for silicon cells, lacked a thorough analysis of this problem.

After the diode ideality factors have been set to $n_1 = 1$ and $n_2 = 2$ to account for diffusion and recombination currents respectively, the double-diode model of the PV cell consists of five parameters. The cell's data sheet values V_{oc},I_{sc},V_m, and I_m yield four independent equations (three data points of the IV-curve and its derivative at MPP), thus allowing to express four of these parameters (R_{sh},I_{ph},I_{s_1},I_{s_2}) as functions of the last (R_s). The positivity of all model parameters, which is a physical necessity, can be exploited to further delimit the possible range of the parameters.

Thus, if V_{oc},I_{sc},V_m, and I_m are known the formulas presented in this contribution give boundaries within which the double diode parameters must lie with certainty. These

boundaries can be used to restrict the search region or provide suitable initial values for fitting procedures if additional IV-curve data points are available.

If no additional data are available various methods can be exploited to guess the double diode parameters. In the most simple approach, the remaining parameter R_s is arbitrarily chosen within the physically allowed range. Alternatively, an approximate fifth condition can be demanded to hold exactly yielding a nonlinear equation for R_s. The different methods are tested for cells whose double diode parameters are known, either from literature or from fits to full IV-curve data. These "approved" parameters are compared to the extracted. Two error measures have been introduced, accounting for the accuracy of either parameter or IV-curve reproduction. As benchmark for the newly introduced methods, an adapted version of an elsewhere published method relying on approximating the slope of the IV-curve at short-circuit is included in the evaluation. Taking the medium value of R_s within the allowed range and calculating the other parameters already gives better results than this method for both error measures and does not require the solution of an additional equation. Its performance can be surpassed by a newly derived approach relying on approximating the slope of a secant in the vicinity of the short circuit point with the slopes of the tangents of its endpoints. In particular, for modern cells with high-quality production standards and therefore presumably high-shunt resistances accurate parameter guesses are possible and the new method provides an automated procedure for a reliable parameter extraction from cell data sheet values only.

When cells are connected to modules an exact calculation of the maximum power output requires the knowledge of the full IV-curves of the constituent single cells. The actual values of the double diode parameters are less important in this case. The parameter set gained from the lowest possible value of R_s yields a further reduced curve reproduction error compared to the 2tangs-method, though it is often accompanied by an unphysical, infinite shunt resistance. Since no additional equation has to be solved, an easily implementable, fast algorithm to obtain reliable IV-curves from cell data sheet values only is achieved.

ACKNOWLEDGMENTS

The authors would like to thank A. Malinge and E. Terrace from the S'tile company[2] in Poitiers, France for providing the full IV-curve of the case study cell. This work was supported by the EU-horizon 2020 project ID 737884.

CONFLICT OF INTEREST

None declared.

ENDNOTES

[1]https://setis.ec.europa.eu/european-industrial-initiative-solar-energy-photovoltaic-energy

[2]http://silicontile.fr/en/

REFERENCES

1. Haegel NM, Margolis R, Buonassisi T, et al. Terawatt-scale photovoltaics: trajectories and challenges. *Science*. 2017;356:141-143.
2. van Overstraeten R, Mertens R. *Physics, Technology and Use of Photovoltaics*. Boca Raton, FL: Taylor & Francis; 1986.
3. Fahrenbruch A, Bube R. *Fundamentals of Solar Cells: Photovoltaic Solar Energy Conversion*. New York, NY: Academic Press; 1983.
4. Datta SK, Mukhopadhyay K, Bandopadhyay S, Saha H. An improved technique for the determination of solar cell parameters. *Solid-State Electron*. 1992;35:1667-1673.
5. Chegaar M, Azzouzi G, Mialhe P. Simple parameter extraction method for illuminated solar cells. *Solid-State Electron*. 2006;50:1234-1237.
6. Chegaar M, Ouennoughi Z, Hoffmann A. A new method for evaluating illuminated solar cell parameters. *Solid-State Electron*. 2001;45:293-296.
7. Easwarakhanthan T, Bottin J, Bouhouch I, Boutrit C. Nonlinear minimization algorithm for determining the solar cell parameters with microcomputers. *Int J Sol Energy*. 1986;4:1-12.
8. Enebish N, Agchbayar D, Dorjkhand S, Baatar D, Ylemj I. Numerical analysis of solar cell current-voltage characteristics. *Sol Energy Mater Sol Cells*. 1993;29:201.
9. Hovinen A. Fitting of the solar cell IV-curve to the two diode model. *Phys Scr*. 1994;1994:175-176.
10. Charles JP, Bordure G, Khoury A, Mialhe P. Consistency of the double exponential model with physical mechanisms of conduction for a solar cell under illumination. *J Phys D: Appl Phys*. 1985;18:2261-2268.
11. Hejri M, Mokhtari H, Azizian MR, Ghandhari M, Söder L. On the parameter extraction of a five-parameter double-diode model of photovoltaic cells and modules. *IEEE J Photovolt*. 2014;4:915-923.
12. Protogeropoulos C, Brinkworth BJ, Marshall RH, Cross BM. *Evaluation of Two Theoretical Models in Simulating the Performance of Amorphous – Silicon Solar Cells*. Dordrecht: Springer Netherlands; 1991:412-415.
13. Garrido-Alzar C. Algorithem for extraction of solar cell parameters from I-V curve using double experimental model. *Renewable Energy*. 1997;10:125-128.
14. Cotfas D, Cotfas P, Kaplanis S. Methods to determine the dc parameters of solar cells: a critical review. *Renew Sustain Energy Rev*. 2013;28:588-596.
15. Chan DSH, Phang JCH. Analytical methods for the extraction of solar-cell single- and double-diode model parameters from I-V characteristics. *IEEE Trans Electron Devices*. 1987;34:286-293.
16. Soto WD, Klein S, Beckman W. Improvement and validation of a model for photovoltaic array performance. *Sol Energy*. 2006;80:78-88.
17. Boyd MT, Klein SA, Reindl DT, Dougherty BP. Evaluation and validation of equivalent circuit photovoltaic solar cell performance models. *J Sol Energy Eng*. 2011;133:021005.

18. Gow JA, Manning CD. Development of a photovoltaic array model for use in power-electronics simulation studies. *IEE Proc Electr Power Appl*. 1999;146:193.
19. Suckow S, Pletzer TM, Kurz H. Fast and reliable calculation of the two-diode model without simplifications. *Prog Photovoltaics Res Appl*. 2014;22:494-501.
20. Shockley W, Read WT. Statistics of the recombinations of holes and electrons. *Phys Rev*. 1952;87:835-842.
21. Hall RN. Electron-hole recombination in germanium. *Phys Rev*. 1952;87:387.
22. Quaschning V. *Regenerative Energiesysteme: Technologie - Berechnung - Simulation*. Munich: Carl Hanser Verlag GmbH & Company KG; 2015.
23. Breitenstein O, Rakotoniaina JP, Al Rifai MH, Werner M. Shunt types in crystalline silicon solar cells. *Prog Photovoltaics Res Appl*. 2004;12:529-538.

How to cite this article: Sulyok G, Summhammer J. Extraction of a photovoltaic cell's double-diode model parameters from data sheet values. *Energy Sci Eng*. 2018;00:1–11. https://doi.org/10.1002/ese3.216

APPENDIX A: Silicon cell under different temperature and illumination conditions

The double diode parameters in the following tables are taken from[10] where a 2×2 cm2 silicon cell has been investigated under different temperature and illumination conditions. From these double diode parameters, the electrical circuit parameters V_{oc},I_{sc},V_m, and I_m are calculated and fed into the different extraction methods yielding new double diode parameter sets. The quality of the methods is quantified by the error measures E_1 and E_2 related either to parameter or to IV-curve reproduction accuracy.

TABLE A1 Double diode parameters and error measures for the cell studied in[10] under AM1 illumination and with T = 299.4∘K. The corresponding electrical circuit parameters fed into the algorithms are $I_{sc} = 117.5$ mA, $V_m = 470.7$ mV, $I_m = 108.0$ mA, and $V_{oc} = 583.7$ mV yielding a fill factor of 74.13%

	Literature	R_s^{half}	$1/R_{sh}$	2tangs	R_s^{low}
Parameters					
R_s [mΩ]	264	305	323	276	256
R_{sh} [Ω]	2550	352	239	977	∞
I_{ph}[mA]	117.5	117.6	117.6	117.5	117.5
I_{s_1}[nA]	0.0129	0.0147	0.0155	0.0134	0.0126
I_{s_2}[μA]	0.38	0.22	0.14	0.33	0.41
Errors					
E_1[%]	0.0	31.7	39.3	16.4	∞
E_2 [‰]	0.0	1.88	2.84	0.49	0.31

TABLE A2 Double diode parameters and error measures for the cell studied in [10] under AM1 illumination and with T = 317.5∘K. The corresponding electrical circuit parameters fed into the algorithms are $I_{sc} = 121.3$ mA, $V_m = 415.8$ mV, $I_m = 109.7$ mA, and $V_{oc} = 529.1$mV yielding a fill factor of 71.11%

	Literature	R_s^{half}	$1/R_{sh}$	2tangs	R_s^{low}
Parameters					
R_s [mΩ]	272	310	338	292	265
R_{sh} [Ω]	2040	258	140	459	∞
I_{ph} [mA]	121.3	121.4	121.6	121.4	121.3
I_{s_1} [nA]	0.0352	0.0402	0.0442	0.0378	0.0344
I_{s_2} [μA]	2.08	1.18	0.45	1.61	2.23
Errors					
E_1 [%]	0.0	31.7	44.4	22.9	∞
E_2 [‰]	0.0	1.36	2.60	0.69	0.21

TABLE A3 Double diode parameters and error measures for the cell studied in [10] under AM1 illumination and with T = 330∘K. The corresponding electrical circuit parameters fed into the algorithms are $I_{sc} = 123.3$ mA, $V_m = 379.4$ mV, $I_m = 109.9$ mA, and $V_{oc} = 491.8$ mV yielding a fill factor of 68.78%

	Literature	R_s^{half}	$1/R_{sh}$	2tangs	R_s^{low}
Parameters					
R_s [mΩ]	272	306	341	294	260
R_{sh} [Ω]	910	200	99	288	∞
I_{ph} [mA]	123.3	123.5	123.7	123.4	123.3
I_{s_1} [nA]	2.72	3.09	3.50	2.95	2.60
I_{s_2} [μA]	6.08	3.65	9.42	4.55	6.85
Errors					
E_1 [%]	0.0	28.9	45.6	22.0	∞
E_2 [‰]	0.0	1.01	2.27	0.62	0.30

TABLE A4 Double diode parameters and error measures for the cell studied in [10] with T = 320.8∘K and illumination of 140% AM1. The corresponding electrical circuit parameters fed into the algorithms are $I_{sc} = 162.8$ mA, $V_m = 409.2$ mV, $I_m = 145.8$ mA, and $V_{oc} = 532.8$ mV yielding a fillfactor of 68.76%

	Literature	R_s^{half}	$1/R_{sh}$	2tangs	R_s^{low}
Parameters					
R_s [mΩ]	271	300	325	287	258
R_{sh} [Ω]	625	163	89	259	∞
I_{ph} [mA]	162.9	163.1	163.4	163.0	162.8
I_{s_1} [nA]	0.47	0.55	0.61	0.51	0.44
I_{s_2} [μA]	3.32	2.06	0.87	2.66	3.84
Errors					
E_1 [%]	0.0	27.6	41.9	18.5	∞
E_2 [‰]	0.0	1.13	2.33	0.57	0.42

TABLE A5 Double diode parameters and error measures for the cell studied in[10] with T = 316.5∘K and illumination of 40% AM1. The corresponding electrical circuit parameters fed into the algorithms are $I_{sc} = 44.7$ mA, $V_m = 403.9$ mV, $I_m = 40.3$ mA, and $V_{oc} = 500.5$ mV yielding a fill factor of 72.85%

	Literature	R_s^{half}	$1/R_{sh}$	2tangs	R_s^{low}
Parameters					
R_s [mΩ]	317	400	513	324	255
R_{sh} [Ω]	1700	641	304	1521	∞
I_{ph} [mA]	44.7	44.7	44.8	44.7	44.7
I_{s_1} [nA]	0.345	0.384	0.441	0.348	0.317
I_{s_2} [μA]	1.26	0.83	0.20	1.23	1.56
Errors					
E_1 [%]	0.0	26.8	51.3	3.2	∞
E_2 [‰]	0.0	1.20	3.20	0.09	0.76

For the cell studied in Ref.,[10] the 2tangs-method is most suited to reproduce the double diode parameters for all investigated combinations of temperature and illumination. The most reliable reproduction of the IV-curve is obtained from the R_s^{low}-method. This suggests that the results from the standard testing conditions (25∘C, 1000 W/m2) for a silicon cell can be extrapolated to other temperature and illumination levels.

APPENDIX B: TL1-900-50 cell parameters

The following double diode parameters are from a 3-in-diameter silicon cell labeled TL1-900-50 and measured in Ref.[15] Original and reproduced double diode parameters are listed in Table B1. In contrast to the other investigated cells, the 2tangs-method has the largest parameter reproduction error E_1. The value of R_s found from the 2tangs-method's condition Equation (33) is de facto identical to the lowest possible value of R_s. In that case, the double diode parameters obtained from the 2tangs-method have to be treated with care. However, the reproduction of the IV-curve in the vicinity of the maximum power point expressed by error measure E_2 is still more reliable than for the $1/R_{sh}$-method.

TABLE B1 Double diode parameters and error measures for the TL1-900-50 cell studied in [15] with T = 323.15∘K and under AM1 illumination. The corresponding electrical circuit parameters fed into the algorithms are $I_{sc} = 905.8$mA, $V_m = 414.6$ mV, $I_m = 792.3$ mA, and $V_{oc} = 531.7$ mV yielding a fillfactor of 68.2%

	Literature	R_s^{half}	$1/R_{sh}$	**2tangs**	R_s^{low}
Parameter					
R_s [mΩ]	31.17	26.14	44.74	7e-4	0
R_{sh} [Ω]	19.92	24.80	10.32	46.41	46.41
I_{ph} [A]	0.9072	0.9067	0.9097	0.9058	0.9058
I_{s_1} [nA]	2.466	2.091	3.564	0.215	0.737
I_{s_2}[μA]	28.31	33.91	11.33	60.83	60.83
Errors					
E_1 [%]	0.0	15.13	39.30	87.86	87.86
E_2 [‰]	0.0	0.61	2.55	1.91	1.91